An ultimate-high linear silicon modulator based on all-optical linearization method

Jingyang Fan[1], Qiang Zhang[2*], Shengyu Fang[1], Xingyi Jiang[1], Shuyue Zhang[1], Hui Yu[2]
[1]*College of Information Science and Electronic Engineering, Zhejiang University, Hangzhou 310027, China*
[2]*Zhejiang Lab, Hangzhou 311121, China*
**Corresponding author: zhangqiang@zhejianglab.com*

Abstract: We proposed an ultimate-high linear silicon-based modulator based on all-optical linearization method, which demonstrates an SFDR as high as 131/127 dB·Hz$^{6/7}$ at 1/10 GHz.

OCIS codes:(130.0130) Integrated optics; (060.5625) Radio frequency photonics

1. Introduction

Photonics integration on a silicon-on-insulator (SOI) substrate is a promising strategy in high-speed communication and high-performance computing systems [1-2], since its CMOS compatibility, high integration density and potential of seamless integration with electronics devices. Besides, it also motivates the development of integrated microwave photonics (IMWP) links and systems where microwave signals are processed in the optical domain. In an IMWP system, linearity is a key metric which is often characterized by the carrier-to-distortion ratio (CDR) or spurious-free dynamic range (SFDR), determining its systematic performance [3]. It is known that, silicon-based electro-optical (EO) modulator introduces a strong nonlinearity to such IMWP systems since the carrier-depletion effect. Recently, two works demonstrate ultra-high linear silicon-based Mach-Zehnder modulators (MZMs), which achieve the SFDRs over 120 dB·Hz$^{2/3}$ [4-5]. The linearization principle in [4] is to manipulate power distribution of RF and optical signals among two sub-MZMs; thus, the nonlinearities in such two sub-MZMs can cancel each other. Similarly, in [5], the nonlinear responses of two PN-junction-based phase shifters in an MZM can be suppressed by tuning the bias voltages and driving powers. As it can be seen that, the two linearization methods still require electrical processing of modulation signals, increasing the complexity and power consumption while reducing the operation bandwidth and tuning flexibility of systems. In this work, we proposed an all-optical linearization scheme based on a novel dual-series MZM architecture. The measured record-high SFDR for the third-order inter-modulation distortion (IMD3) are as high as 131/127 dB·Hz$^{6/7}$ at 1/10 GHz.

2. Device Architecture & Linearization Principle

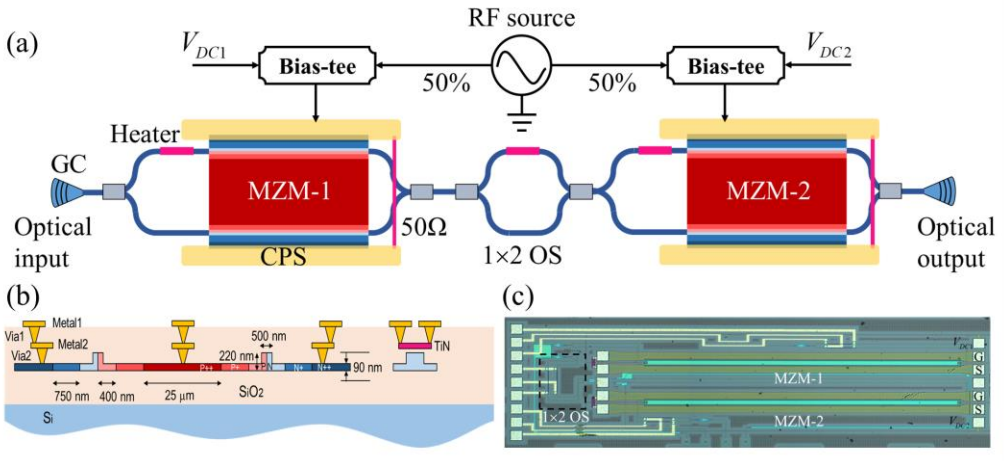

Fig. 1(a) Schematic diagram of the proposed silicon dual-series MZM. (b) Cross-sectional views of the PN junction and the heater of the silicon MZMs. (c) Microscope image of the silicon dual-series MZM.

A schematic diagram and a microscope image of our device are shown in Figs. 1(a) and 1(c), respectively. It composed of two silicon carrier-depletion-based MZ modulators which are connected in series. A 1×2 optical switch (OS) is integrated with the second sub-MZM for tuning its extinction ratio (ER). Based on such architecture, adjusting

ER of the second sub-MZM can be seen as tuning the RF power splitting ratio of the two sub-MZMs. Subsequently, the third-order intermodulation distortions generated from the two MZMs can cancel each other out by a proper ER when they are biased at two quadrature points with opposite polarities.

As shown in Fig. 1(a), each sub-MZM is comprised of two 2-mm-long active waveguides and ground-signal electrode. An on-chip terminator with TiN-based 50 Ω resistance is connected to the end of the RF electrode in each sub-MZM. The doping concentration of the PN junction varies from 0.8×10^{18}cm^{-3} to 1.5×10^{18}cm^{-3} in vertical direction while the doping concentrations of intermediate P+ and N+ regions are 2×10^{18} cm^{-3}. On the other hand, the ohmic contact regions are heavily doped to 10^{20} cm^{-3} to reduce the contact resistance. It is worth noting that, the two PN junctions are connected in series to increase its modulation bandwidth. TiN-based heaters are used to set bias points of the two sub-MZMs and tune the corresponding ER. Cross-sections of the phase shifter and the heater are shown in Fig. 1(b). Devices are fabricated on the silicon-on-insulator (SOI) wafer with a 220 nm thick silicon layer and a 3 μm thick buried oxide (BOX) in Singapore AMF (Advance Micro Foundry).

The modulation transfer function of the proposed MZM in Fig. 1(a) can be written as

$$I_{out}=\frac{|E_{in}|^2}{16}\left[\begin{array}{l} e^{-2\alpha\left(V_{b1}+\frac{v_{RF}}{2\sqrt{2}}\right)L}+e^{-2\alpha\left(V_{b1}-\frac{v_{RF}}{2\sqrt{2}}\right)L} \\ +2e^{-\left[\alpha\left(V_{b1}+\frac{v_{RF}}{2\sqrt{2}}\right)+\alpha\left(V_{b1}-\frac{v_{RF}}{2\sqrt{2}}\right)\right]L}\cos(\Delta\theta_1)\end{array}\right]\cdot\left[\begin{array}{l}(1+\sin\varphi)e^{-2\alpha\left(V_{b2}+\frac{v_{RF}}{2\sqrt{2}}\right)L}+(1-\sin\varphi)e^{-2\alpha\left(V_{b2}-\frac{v_{RF}}{2\sqrt{2}}\right)L} \\ +2e^{-\left[\alpha\left(V_{b2}+\frac{v_{RF}}{2\sqrt{2}}\right)+\alpha\left(V_{b2}-\frac{v_{RF}}{2\sqrt{2}}\right)\right]L}\cos(\Delta\theta_2)\cos\varphi\end{array}\right] \quad (1)$$

In Eq. (1), $|E_{in}|^2$ represents the power of input optical field, $\alpha(v)$ is the attenuation coefficient of the phase shifter which depends on the driving voltage v on the PN junction. φ denotes the optical phase difference of two arms in the 1×2 OS produced by HT-2. Thus, the corresponding optical power ratio of the 1×2 OS can be expressed as $\beta=(1+\sin\varphi)/2$, and ER can be derived as $-20\lg|(\beta-1)/(\beta+1)|$. V_{b1} and V_{b2} represent the reverse bias voltages of the PN junctions in MZM-1 and MZM-2, respectively. $\Delta\theta_{1/2}$ denote the optical path differences between arms of the sub-MZMs, which can be calculated as $\Delta\theta=\theta_{bias}+2\pi L\Delta n_{eff}(v)/\lambda$. θ_{bias} is the static bias phase produced by the heater, $\Delta n_{eff}(v)$ represents the effective index change induced by the driving voltage v. Here, we assume that the RF power divided equally into the MZM-1 and MZM-2; thus, driving voltages on the two sub-MZMs are $V_{b1}+v_{RF}/2^{0.5}$ and $V_{b2}+v_{RF}/2^{0.5}$. v_{RF} is the amplitude of RF signal from the RF source. MZM-1 and MZM-2 operate at their quadrature points, but with opposite polarities, i.e., $\theta_{bias1}+2\pi L\Delta n_{eff}(V_{b1})/\lambda=\pi/2$, $\theta_{bias2}+2\pi L\Delta n_{eff}(V_{b2})/\lambda=-\pi/2$. According to the nonlinear modulation theory [6], amplitudes of the first harmonic (FH) and the IMD3 components in the modulated optical field can be obtained by calculating derivatives of I_{out} with respect to v_{RF}. With a proper value of the ER, the IMD3 component can be suppressed.

3. Experiments and Results

The two-tone test is implemented to characterize linearities of the devices with the measurement setup shown in Fig. 2. A TE-polarized light from an ultra-low-noise laser (ULN15PC) is coupled into and out of the device by two grating couplers (GCs). The output power and the relative intensity noise (RIN) are 120 mW and -165 dB/Hz, respectively, which is well suitable for ultrahigh-SFDR MWP systems. The two-tone signal is generated by a RF source (Keysight E8267D), and then equally distributed to two paths by a 50/50 RF power splitter. One path is directly fed to MZM-1, and the other path first passes through an electrical phase shifter (EPS) to ensure that the delay of the two paths is equal, then drives the MZM-2.

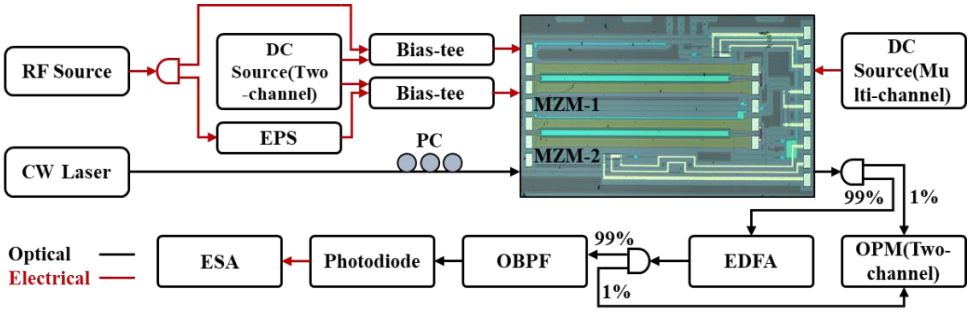

Fig. 2. Setup for the SFDR measurement. EDFA: erbium doped fiber amplifier; OBPF: optical bandpass filter; ESA: electrical spectrum analyzer; PC: polarization controller; EA: electrical attenuator; EPS: electrical phase shifter; OPM: optical power meter.

A two-channel voltage source is used for providing reverse bias voltage of PN junctions in the two sub-MZMs. The reverse bias voltageis combined with the RF driving signals via two bias-tees (SHF BT 65A), which are then fed to two sub-MZMs via a 67 GHz GSSG probe (GGB Industries). Another multi-channel voltage source is employed to drive the heaters for tuning the operation condition of two sub-MZMs. The output of the modulator is amplified by an erbium doped fiber amplifier (EDFA, Keopsys) to compensate for the coupling loss of the two fiber grating couplers (12 dB in total) and the insertion loss of the device. An optical bandpass filter (OBPF WaveShaper 2000A) is used to suppress the amplified spontaneous emission noise (ASE). The optical-to-electrical conversion is performed by a 30 GHz photodiode with a responsivity of 0.75 A/W. The output RF signal of the PD is analyzed by a 90 GHz electrical spectrum analyzer (ESA, N9041B UXA).

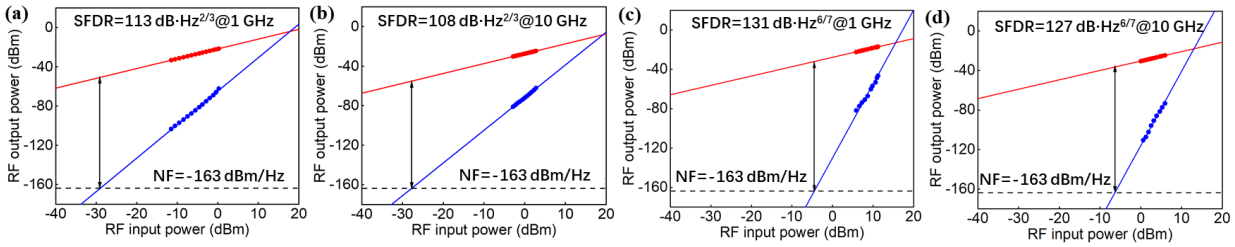

Fig. 3. Measured SFDRs of the reference single MZM and proposed novel dual-series MZM at different frequencies. Reference single MZM at (a) 1 GHz (b) 10 GHz. Novel dual-series MZM at (c) 1GHz (d) 10 GHz.

In order to compare linearities of the single and the dual-series MZMs fairly, their outputs are amplified to 10 dBm. Two 1/99 optical power splitters and a two-channel optical power meter are used to monitor the optical power at the points before and after the EDFA. The first monitoring point enables us to set bias points of sub-MZMs, while the second monitoring point is used to control the output level of the EDFA at 10 dBm during the SFDR measurement. The two tones with a spacing of 1 MHz are centered at 1 GHz or 10 GHz. Since the ultra-low-noise laser with high output power and the ESA with function of preamplification is employed in this system, the noise floor is measured to be -163 dBm/Hz.

As shown in Figs. 3(a) and 3(b), the SFDR of reference single MZM is measured to be 113/108 dB·Hz$^{2/3}$ at 1/10 GHz by optimizing the reverse bias voltage of the PN-junction-based phase shifter to 3.7 V [6]. After that, the dual-series MZM is characterized by biasing both sub-MZMs at quadrature points and the ER of the second sub-MZM. When the value of β is tuned to be ~0.7 (ER ~ 15 dB), SFDRs are improved substantially to 131 dB·Hz$^{6/7}$ and 127 dB·Hz$^{6/7}$ at frequencies of 1 GHz and 10 GHz, respectively. The corresponding measured results are illustrated in the Figs. 3(c) and 3(d).

4. Conclusion

We propose and demonstrate an ultimate-high linear silicon carrier-depletion-based modulator by a novel dual-series MZM architecture and all-optical linearization scheme. By tuning the ER of the second sub-MZM and operation bias points of two sub-MZMs, the modulator achieves a record-high SFDR of 131/127 dB·Hz$^{6/7}$ at 1/10 GHz.

Acknowledgement

The authors would like to thank Dr. Bing Wei, Training Platform of Information and Microelectronic Engineering in Polytechnic Institute of Zhejiang University.

References

[1]. L. Liao, *et al*. “Silicon photonics for next-generation optical connectivity”, 2023 Optical Fiber Communications Conference and Exhibition (OFC). IEEE, 2023.
[2]. D. Liang, *et al*. “An energy-efficient and bandwidth-scalable DWDM heterogeneous silicon photonics integration platform”, IEEE J. Sel. Top. Quantum Electron. **28** (6), 1-19 (2022).
[3]. D. Marpaung, et al. “Integrated microwave photonics”, Laser Photonics Rev., **7**(4), 506-538 (2013).
[4]. H. Yue, *et al*. “Ultrahigh-linearity dual-drive scheme using a single silicon modulator”, Opt. Lett., **48**(11), 2995-2998 (2023).
[5]. Q. Zhang, *et al*. “High linearity silicon modulator capable of actively compensating input distortion”, Opt. Lett., **45**(13), 3785-3788 (2020).
[6]. Q. Zhang, *et al*. “Linearity Comparison of Silicon Carrier-Depletion-Based Single, Dual-Parallel, and Dual-Series Mach–Zehnder Modulators”, J. Lightwave Technol. **36** (16), 3318-3331 (2018).